Research

Prefrontal consolidation supports the attainment of fear memory accuracy

Philip A. Vieira,[1] Jonathan W. Lovelace,[1] Alex Corches,[2] Asim J. Rashid,[3]
Sheena A. Josselyn,[3] and Edward Korzus[1,2]

[1]Department of Psychology and Neuroscience Program, University of California Riverside, California 92521, USA; [2]Biomedical Sciences Program, University of California Riverside, California 92521, USA; [3]Program in Neurosciences and Mental Health, Hospital for Sick Children, Toronto, Ontario M5G 1X8, Canada

The neural mechanisms underlying the attainment of fear memory accuracy for appropriate discriminative responses to aversive and nonaversive stimuli are unclear. Considerable evidence indicates that coactivator of transcription and histone acetyltransferase cAMP response element binding protein (CREB) binding protein (CBP) is critically required for normal neural function. CBP hypofunction leads to severe psychopathological symptoms in human and cognitive abnormalities in genetic mutant mice with severity dependent on the neural locus and developmental time of the gene inactivation. Here, we showed that an acute hypofunction of CBP in the medial prefrontal cortex (mPFC) results in a disruption of fear memory accuracy in mice. In addition, interruption of CREB function in the mPFC also leads to a deficit in auditory discrimination of fearful stimuli. While mice with deficient CBP/CREB signaling in the mPFC maintain normal responses to aversive stimuli, they exhibit abnormal responses to similar but nonrelevant stimuli when compared to control animals. These data indicate that improvement of fear memory accuracy involves mPFC-dependent suppression of fear responses to nonrelevant stimuli. Evidence from a context discriminatory task and a newly developed task that depends on the ability to distinguish discrete auditory cues indicated that CBP-dependent neural signaling within the mPFC circuitry is an important component of the mechanism for disambiguating the meaning of fear signals with two opposing values: aversive and nonaversive.

The ability to discriminate between similar, yet different, stimuli is critical for cognitive functioning (O'Reilly and McClelland 1994) and is referred to as memory specificity or memory accuracy. Failure to discriminate between aversive and nonaversive stimuli during recall may indicate decreased memory resolution (i.e., reduced access to memory details) or generalized fear or both, and may lead to inappropriate stimulus generalization. Generalization is not always inappropriate and this type of reduced fear memory accuracy is observed when one responds the same to two stimuli that are not identical. After initial generalization, fear memory accuracy can be increased through additional experiences with reinforced aversive stimulus and nonreinforced nonaversive stimulus. Conversely, overgeneralized fear is a typical symptom of anxiety disorders including phobias and post-traumatic stress disorder (PTSD), which are triggered by cues resembling traumatic experience in a secure environment (Mahan and Ressler 2012). Studies of neural substrates and mechanisms underlying memory resolution are focused on the hippocampal circuit (Leutgeb et al. 2007; Sahay et al. 2011). Recent studies also implicate prefrontal circuitry in the contextual fear memory specificity and generalization (Xu et al. 2012; Xu and Sudhof 2013) or discrimination of more discrete multiple odor stimuli (DeVito et al. 2010).

Regulatory mechanisms direct cAMP response element binding protein (CREB)-dependent transcription subsequent to learning-induced molecular changes in which neurons play a pivotal role in the conversion of short-term to long-term memory across species (Dash et al. 1990; Bourtchuladze et al. 1994; Yin et al. 1994; Josselyn et al. 2001; Kida et al. 2002; Pittenger et al.

2002). Phosphorylation of CREB at serine 133 is required for the recruitment of the chromatin remodeling factor with intrinsic acetyltransferase activity CREB binding protein (CBP), both events critical for CREB-dependent transcription (Gonzalez et al. 1989; Chrivia et al. 1993). CBP integrates multiple signaling pathways via direct interactions with independently regulated multiple transcriptional factors and components of transcriptional machinery. In addition, CBP comprises enzymatic activity referred to as HAT (histone acetyltransferase), which enables acetylation of conserved lysine amino acids on proteins by catalyzing the transfer of an acetyl group of acetyl CoA to form ε-N-acetyl-lysine (Bannister and Kouzarides 1996; Korzus et al. 1998). Initially, histones were considered as primary natural substrates for CBP enzymatic activity. However, histones are not the only targets for CBP's HAT activity and a number of nonhistone potential targets for CBP's HAT activity have been found, including proteins regulating chromatin remodeling and gene expression such as p53 (Gu and Roeder 1997), CREB (Lu et al. 2003), and many others (Kouzarides 2000; Sterner and Berger 2000; Yang 2004; Glozak et al. 2005; Kimura et al. 2005). Impact of histone and nonhistone protein acetylation by CBP is not fully understood. Despite uncertainty in respect to how CBP controls neuronal function via its interaction with multiple regulatory proteins and acetyltransferase activity, considerable evidence indicates that CBP is a critical component of the neural signaling underlying cognitive functioning (Alarcon et al. 2004; Korzus et al. 2004; Wood et al.

2005; Chen et al. 2010; Barrett et al. 2011; Valor et al. 2011, 2013; Peixoto and Abel 2012; Maddox et al. 2013). However, it is difficult to separate developmental defects, compensatory developmental effects, and acute function in the adult brain of a gene with pronounced developmental functions. To avoid developmental confounds, four independent manipulations to down-regulate CBP acetyltransferase activity specifically in the adult living brain have been reported to date. Acute CBP hypofunction targeted specifically in adult mice by means of Tet-regulatable expression of CBPΔHAT targeted to excitatory forebrain neurons (Korzus et al. 2004) or hippocampal focal knockout of CBP (Barrett et al. 2011) or intra lateral amygdala infusion of c646, a selective pharmacological inhibitor of p300/CBP activity, shortly following fear conditioning (Maddox et al. 2013) resulted in selective impairment of long-term potentiation (Barrett et al. 2011; Maddox et al. 2013) and long-term memory (Korzus et al. 2004; Barrett et al. 2011; Maddox et al. 2013). In addition, ablation of CBP in the adult brain resulted in impaired environmental enrichment-induced neurogenesis (Lopez-Atalaya et al. 2011), which suggests an additional role of CBP in adult neurogenesis-dependent enhancement of adaptability toward novel experiences (Aimone et al. 2011; Sahay et al. 2011). These data strongly implicate CBP acetyltransferase activity in neural epigenetic signaling underlying long-term memory consolidation.

Although there has been extensive research into the function of the PFC during information acquisition and retrieval, a fundamental question that has escaped resolution is whether CBP-dependent signaling within the prefrontal cortex supports mechanisms in which fear memories are encoded and retrieved without confusion. Using mutant mice expressing dominant negative CBP with eliminated acetyltransferase activity, we have tested the impact of CBP-dependent mechanisms in the mPFC on fear memory accuracy. Evidence from context and auditory discriminatory tasks indicated that the mPFC circuitry is critical for the acquisition of fear memory accuracy necessary for the recognition of subtle differences between aversive and nonaversive stimuli. These data indicate that CBP-dependent signaling in the mPFC is critical for the suppression of fear responses to nonrelevant stimuli, which is a necessary process toward improvement of fear memory accuracy.

Results

Impairment of contextual fear memory specificity in CBPΔHAT[PFC] mice

The CBPΔHAT mutant, a dominant-negative inhibitor of CBP-dependent lysine acetylation, harbors a substitution mutation of two conserved residues (Tyr^{1540}/Phe^{1541} to Ala^{1540}/Ala^{1541}) in the acetyl CoA binding domain (Korzus et al. 1998, 2004). This mutant has no intrinsic acetyltransferase activity due to its inability to interact with a donor of acetyl group, acetyl-CoA, but it retains all protein–protein interaction domains (Korzus et al. 1998). When expressed acutely in adult excitatory neurons, CBPΔHAT functions as a specific blocker of long-term memory consolidation without affecting information acquisition or short-term memory (Korzus et al. 2004). To test the impact of CBP-dependent signaling in the medial prefrontal cortex (mPFC) on fear memory specificity, we generated mice expressing CBPΔHAT and eGFP in the mPFC using virus-mediated gene transfer (referred to as CBPΔHAT[PFC] mice) (Fig. 1A). For control mice, we injected virus-expressing eGFP only in the mPFC. Cytohistological analysis of brain tissue isolated from CBPΔHAT[PFC] and control animals revealed that the majority of cells expressing mutant protein in the mPFC were neurons (Ctrl, 93.85 ± 0.006%, $n = 3$;

CBPΔHAT[PFC], 92.06 ± 0.012%, $n = 3$; $t_{(2)} = -0.03$, $P = 0.511$, $r = 0.013$; data not shown). Conditioned CBPΔHAT[PFC] mice display decreased levels of acetylated histone H3 (t-test, $t_{(10)} = 2.38$, $P = 0.0382$, $r = 0.6013$; Ctrl, 1 ± 0.06, $n = 5$; CBPΔHAT[PFC], 0.74 ± 0.06, $n = 7$) and acetylated histone H4 (Ac-H4 [right panel], t-test, $t_{(10)} = 2.9718$, $P = 0.0140$, $r = 0.6848$; Ctrl, 1 ± 0.04, $n = 6$; CBPΔHAT[PFC], 0.67 ± 0.10, $n = 6$) in cells expressing GFP when compared to conditioned control animals (Fig. 1B). These data are consistent with previous studies reporting decreased levels of acetylated histones in CBP mutant mice (Alarcon et al. 2004; Wood et al. 2005; Chen et al. 2010; Barrett et al. 2011; Valor et al. 2011; Peixoto and Abel 2012).

We examined CBPΔHAT[PFC] mice using the fear-conditioning paradigm (Fig. 1C). CBPΔHAT[PFC] mice performed similarly to controls in the contextual version of the fear conditioning task after a 24-h delay (Ctrl, 25.78%, $n = 10$; CBPΔHAT[PFC], 22.14%, $n = 10$; $t_{(18)} = 1.28$, $P = 0.108$) (Fig. 1C). To determine whether the mPFC supports fear memory accuracy, we examined CBPΔHAT[PFC] mice using the context fear discrimination task (Fig. 1D; Lovelace et al. 2014). First, we tested CBPΔHAT[PFC] and control mice on a generalization task, in which we examined the freezing responses to novel context B after training on the fear conditioning task to context A. Context B was similar yet not identical to the training context A (see Materials and Methods). We found no difference in freezing responses to context B or A in CBPΔHAT[PFC] and control mice (Context A vs. B t-test: Ctrl, $n = 9$, $P = 0.805$; CBPΔHAT[PFC], $n = 11$, $P = 0.851$) (Fig. 1E). Thus, CBPΔHAT[PFC] mice did not demonstrate any obvious abnormalities in fear memory generality during the initial presentation of novel context B. Next, CBPΔHAT[PFC] mice and control littermates were trained to distinguish between the conditioned context A, which was paired with a foot shock (CS+), and an unconditioned context B, which was not paired with any reinforcement (CS−), over multiple training sessions (Fig. 1D). This task requires temporal integration because animals learn subtle differences between context A and B over many days with a single exposure to each context only once per day. Initially, the control and CBPΔHAT[PFC] mice generalized their conditioned responses and exhibited similar freezing levels to both the CS+ and CS− contexts (Block Trials 1–4). However, the control animals began to freeze significantly less in response to context B compared to context A after four block trials of training, demonstrating the ability to consistently distinguish between similar yet different contexts (Block Trials 5–6) (RM-ANOVA of trial block and context: Context, $F_{(1,8)} = 9.423$, $P = 0.015$; Trial Block, $F_{(5,40)} = 3.24$, $P = 0.015$; Trial Block × Context, $F_{(5,40)} = 6.58$, $P = 0.0001$; $n = 9$) (Fig. 1F). Post hoc analysis using Bonferroni correction for multiple comparisons indicated that differences were present during Trial Blocks 5 ($P = 0.003$) and 6 ($P = 0.005$). In contrast to the control animals, CBPΔHAT[PFC] mice failed to distinguish between context A and B and continued to generalize their conditioned responses throughout all 12 d of training (RM-ANOVA of trial block and context: Context, $F_{(1,10)} = 5.42$, $P = 0.04$; Trial Block, $F_{(2,15)} = 11.09$, $P = 0.002$; Trial Block × Context, $F_{(3,27)} = 1.62$, $P = 0.21$; $n = 11$) (Fig. 1G). These data demonstrated that CBPΔHAT expressed in the mPFC resulted in imbalanced neural processes underlying fear memory specificity and generalization. Analysis of the context discrimination ratio confirmed that at the end of the training, the control animals performed better on the context discrimination task compared to the CBPΔHAT[PFC] mice. Figure 1H shows no difference in performance between control and CBPΔHAT[PFC] animals on Trial Block 1 (t-test, $t_{(18)} = 0.02$, $P = 0.99$, $r = 0.005$), but a marked difference on Trial Block 6 (t-test, $t_{(18)} = 2.60$, $P = 0.018$, $r = 0.52$). These findings demonstrate that CBPΔHAT[PFC] mice have a strong deficit in context discrimination.

Hypothetically, learning of appropriate responses to fearful and similar but not relevant stimuli may involve changes in response to aversive stimuli or nonaversive or both across the entire training. Therefore we analyzed fear responses to Context A (CS+) and, separately, to Context B (CS−) in CBPΔHAT^{PFC} and control mice. There was no difference in responses to conditioned stimuli CS+ between CBPΔHAT^{PFC} and control mice across the entire context discrimination training (RM-ANOVA of Trial Blocks 1–5 and group: Trial Block × Group, $F_{(2.7,47.9)} = 1.782$, $P = 0.169$) (Fig. 1F,G). However, CBPΔHAT^{PFC} and control mice responded differently to nonrelevant stimuli CS− across training on the context discriminatory task (RM-ANOVA of Trial Blocks 1–5 and group: Trial Block × Group, $F_{(2.9,51.6)} = 4.919$, $P = 0.005$) (Fig. 1F,G). Change in freezing to CS− across the training (freezing Δ) was significantly higher in CBPΔHAT^{PFC} when compared to control mice (t-test, $t_{(18)} = −2.235$, $P = 0.038$) (Fig. 1I). However, calculations of freezing Δ consider only performance on Trial Blocks 1 and 6. In order to include performance of tested animals on each day across the entire training on the contextual discriminatory task (Trial Blocks 1–6) (Fig. 1F,G), we compared average slopes (α) of fitted learning curves (Fig. 1J). The learning of appropriate responses to CS+ shows a positive slope in both control (α = 4.76 ± 1.07, where α = slope) and CBPΔHAT^{PFC} (α = 6.35 ± 1.61) mice and there is no difference between groups (t-test, $t_{(18)} = −0.778$, $P = 0.446$). The learning of appropriate response to CS− shows a negative slope in the control group (α = −0.88 ± 1.34), which significantly improved fear memory accuracy at the end of training (Fig. 1F). In contrast, the CBPΔHAT^{PFC} group, which failed to improve fear memory accuracy across training (Fig. 1G), showed a positive slope for CS− (α = 4.26 ± 1.4), a marked difference from control responses to the CS− (CS−/Ctrl, α = −0.88 ± 1.34; CS−/CBPΔHAT^{PFC}, α = 4.26 ± 1.4; CS− slope/Ctrl vs. CBPΔHAT^{PFC} t-test, $t_{(18)} = −2.614$, $P = 0.018$). In summary, analysis of patterns of responses to Context A (CS+) and Context B (CS−) in control animals revealed that the improvement of contextual fear memory accuracy was due to increased freezing behavior to the CS+ and a decrease in freezing to CS−. CBP hypofunction in the mPFC altered the ability to learn discriminatory responses to CS+ vs. CS− by disrupting the pattern of the learning curve for CS− only. These data suggest that the mPFC supports the improvement of contextual fear memory accuracy by controlling the acquisition of appropriate responses to nonrelevant stimuli.

We also found that CBPΔHAT^{PFC} mice performed similar to controls in the cued version of the fear conditioning task during acquisition (data not shown, $F_{(5,90)} = 1.49$, $P = 0.201$) and after a 24-h delay (Ctrl, 47.17 ± 5.82%, n = 10; CBPΔHAT^{PFC}, 57.27 ± 7.21%, n = 10; $t_{(18)} = −1.042$, $P = 0.324$, $r = −0.096$)

(Fig. 2A). These data indicate that information acquisition and long-term memory examined with a 24-h delay on contextual (Fig. 1C) and cued fear-conditioning (Fig. 2A [and also see Fig. 4A,B]) were normal in CBPΔHAT^{PFC} mice. The normal performance of CBPΔHAT^{PFC} on these fear-conditioning tasks (Figs. 1C and 2A [and also see Fig. 4A,B]) indicates that CBPΔHAT^{PFC} mice have functioning circuitry underlying Pavlovian conditioning.

CBPΔHAT^{PFC} mice showed normal levels of locomotor activity (Total Distance Traveled: Ctrl, 46159.94 ± 1335 mm, n = 12; CBPΔHAT^{PFC}, 43563.67 ± 4730.60 mm, n = 16; $t_{(11)} = −0.43$, $P = 0.6627$, $r = 0.1289$. Average Velocity: Ctrl, 51.52 ± 1.50 mm/sec, n = 12; CBPΔHAT^{PFC}, 48.43 ± 5.23 mm/sec, n = 16; $t_{(11)} = −0.367$, $P = 0.6399$, $r = 0.1101$) (Fig. 2B,C) and normal anxiety-related responses (Thigmotaxis: Ctrl, 58.58 ± 4.12%, n = 12; CBPΔHAT^{PFC}, 66.37 ± 6.14%, n = 16; $t_{(11)} = 0.34$, $P = 0.3689$, $r = 0.1030$) (Fig. 2D).
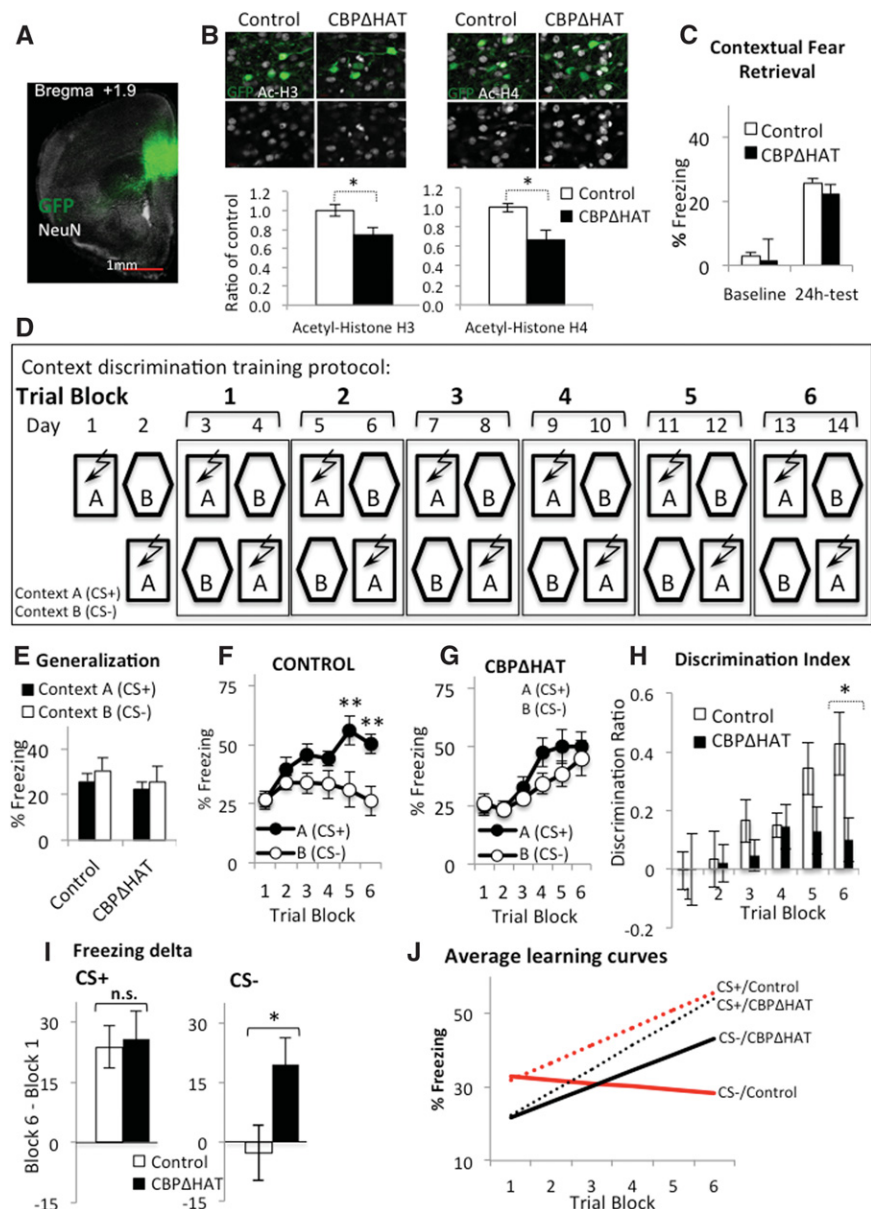

Figure 1. (Legend on next page)

Impairment of auditory memory specificity in CBPΔHAT^{PFC} mice

To evaluate if the deficient discrimination of aversive and nonaversive external stimuli was sensory input-specific, we examined CBPΔHAT^{PFC} mice using a novel auditory discrimination task, which tests the ability of subjects to recognize the direction of frequency modulated (FM)-sweeps (trains of upward and downward FM-sweeps) (Fig. 3). This assay includes 3 d of acquisition (single CS+ foot shock pairing) followed by a 24-h test on Day 4 and a generalization test on Days 4–5. Discrimination training takes place on Days 7–12 in which animals are run through three sessions: first, they are tested for freezing to CS+ and CS− (in context C); second, they are exposed to CS+ (or CS−); third, they are exposed to CS− (or CS+).

In parallel experiments, we also microinjected into the mPFC an HSV virus encoding a mutant form of CREB (mCREB) and tested these mice (mCREB^{PFC}) in the auditory discrimination task. CREB is implicated in memory consolidation across a variety of species (Dash et al. 1990; Bourtchuladze et al. 1994; Yin et al. 1994; Josselyn et al. 2001; Kida et al. 2002; Pittenger et al. 2002) and functions immediately upstream of CBP. mCREB (CREB^{S133A} mutation) cannot be phosphorylated at the key serine 133 residue

and, therefore, cannot recruit CBP and activate transcription (Gonzalez et al. 1989; Chrivia et al. 1993). Thus we have tested a possible involvement of this well-recognized mediator of memory consolidation in auditory fear discrimination in parallel experiments to those performed in CBPΔHAT^{PFC} mice.

We first examined FM-sweep fear conditioning acquisition in CBPΔHAT^{PFC} and mCREB^{PFC} mice. All three groups: the CBPΔHAT^{PFC}, mCREB^{PFC}, and control mice similarly acquired this form of Pavlovian conditioning (RM-ANOVA of Day and Group, $F_{(4,82)} = 0.975$, $P = 0.426$) (Fig. 4A) and showed the same performance on the 24-h memory test (two way ANOVA of Group and Baseline/24 h-Test: Group, $F_{(2,82)} = 0.777$, $P = 0.463$; Baseline/24-h Test, $F_{(1,82)} = 688.3$, $P = 1.2 \times 10^{-41}$; Group × Baseline/24-h Test, $F_{(2,82)} = 0.205$, $P = 0.815$) (Fig. 4B). These data demonstrate that information acquisition and long-term memory tested after a 24-h delay on FM-sweep fear conditioning was normal in CBPΔHAT^{PFC} and mCREB^{PFC} mice. We also tested CBPΔHAT^{PFC}, mCREB^{PFC}, and control mice on generalization tasks, in which we examined their freezing responses to novel downward FM-sweep (CS−) after training on the upward FM-sweep (CS+) fear conditioning task. The generalization test revealed that there was no difference in the freezing responses to the CS− or CS+ between CBPΔHAT^{PFC}, mCREB^{PFC}, and control mice (ANOVA of FM-sweep direction and group during Days 4 and 5: Group, $F_{(2,82)} = 0.37$, $P = 0.692$; ANOVA of FM-sweep direction, $F_{(1,82)} = 3.458$, $P = 0.067$; Group × FM-Sweep Direction, $F_{(2,82)} = 0.090$, $P = 0.914$) (Fig. 4C). These data indicate that strong generalization was observed during Days 4 and 5 in all three tested groups.

Next, the animals underwent auditory discrimination training (Fig. 4D–F). Initially, the control, CBPΔHAT^{PFC} and mCREB^{PFC} mice generalized their conditioned responses and exhibited similar levels of freezing responses to both CS+ and CS− (Days 1–2). However, after 2 d of training, the control animals exhibited a higher number of freezing responses to CS+ and significantly fewer freezing responses to CS− compared to CS+, demonstrating the ability to consistently distinguish between similar yet different auditory patterns (Days 9–12) (RM-ANOVA of Day and FM-sweep direction: Day × FM-sweep direction, $F_{(2.2,33.5)} = 10.776$, $P = 0.0002$, $n = 16$) (Fig. 4D). Post hoc analysis using Bonferroni correction ($\alpha = 0.0083$) for multiple comparisons indicated that differences were present during Days 9 (CS+ vs. CS− t-test, $t_{(30)} = 3.632$, $P = 0.001$, $r = 0.55$), 10 ($t_{(30)} = 5.227$, $P = 0.00001$, $r = 0.69$), 11 ($t_{(30)} = 7.540$, $P = 2.1 \times 10^{-08}$, $r = 0.81$), and 12 ($t_{(30)} = 9.253$, $P = 2.7 \times 10^{-10}$, $r = 0.86$) only.

CBPΔHAT^{PFC} mice demonstrated weak ability to discriminate between CS+ and CS−, and only during the last 2 d of training (RM-ANOVA of Day and FM-sweep direction: Day × FM-sweep direction, $F_{(5,70)} = 5.071$, $P = 0.001$, $n = 15$) (Fig. 4E). Post hoc analysis using Bonferroni correction for multiple

Figure 1. Contextual fear memory specificity was deficient in CBPΔHAT^{PFC} mice. (*A*) Viral-mediated delivery to the mPFC. Long-term expression HSV-1 viruses carrying CBPΔHAT (HSV/CBPΔHAT-IRES2-EGFP) or eGFP as the control (HSV/EGFP) were injected into the mouse mPFC. To determine the pattern of GFP-tagged virus expression, the imaged tissue was compared to the Paxinos and Franklin (2001) mouse atlas and areas of maximal GFP expression were labeled as injection sites. A representative image of mPFC viral infection showed the precision of our viral-targeting procedures. The pattern of EGFP expression was similar 4 d or 20 d after HSV virus injection into the mPFC. Green, GFP; white, NeuN neuronal marker. (*B*) CBPΔHAT blocks acetylation of histone H3 and H4 in the mPFC. To determine the effects of viral infection with CBPΔHAT on neural signaling, the levels of acetylated histones H3 and H4 were assessed in the brains of infected animals and compared to controls in a standard IHC analysis 25 min after auditory fear conditioning (see Materials and Methods). Cells expressing viral CBPΔHAT showed significantly lower levels of acetylated histone H3 and H4 when compared to control animals expressing GFP only. Representative images show GFP (in green) and acetylated histone H3 (Ac-H3, *left* panel; t-test, $t_{(10)} = 2.38$, $P = 0.0382$, effect size $r = 0.6013$) or acetylated histone H4 (Ac-H4, *right* panel; t-test, $t_{(10)} = 2.9718$, $P = 0.0140$, effect size $r = 0.6848$) CBPΔHAT^{PFC} mice. Three animals were used per group. GFP, green; Ac-H3, white; Ac-H4, white; red bar, 10 μm. (*C*) Pavlovian contextual fear conditioning was normal in CBPΔHAT^{PFC} mice. CBPΔHAT^{PFC} and control (Ctrl) mice showed normal acquisition and retention of contextual fear conditioning. Contextual fear was tested in context A at 24 h after a single context A-foot shock pairing. (*D*) Experimental design for the context discrimination test. Context A and B were similar but not identical. The protocol included 14 d of training. The mice were placed in context A (CS+) for 180 sec followed by a foot shock (arrow), and context B (CS−) lacked any reinforcement. (*E*) Generalization test. Freezing behavior to context A and a similar but not identical context B after conditioning to context A-foot shock pairing was not different, in both groups. Freezing in both tested groups was comparable in response to both contexts, indicating that context A was sufficiently similar to context B that generalization was occurring early in training. (*F*) After the initial generalization of fear conditioned responses, control mice exhibited robust fear memory specificity. (*E*) CBPΔHAT^{PFC} mice exhibited a deficit in context discrimination. (*H*) The context discrimination ratios (DI) were calculated using the freezing responses to CS+ and CS− according to the formula DI = ([Context A − Context B]/[Context A + Context B]). Analyses revealed differences in the performance during Trial Block 6 between CBPΔHAT^{PFC} and control mice, but not during Trial Blocks 1–5. CBPΔHAT^{PFC} mice, $n = 11$. Control, $n = 9$. (*I*) Change in freezing across training (freezing Δ), calculated as the (freezing on Trial Block 6 − freezing on Trial Block 1). There was no difference in responses to conditioned stimuli CS+ between CBPΔHAT^{PFC} and control mice. Change in freezing to CS− across the training was significantly higher in CBPΔHAT^{PFC} when compared to control mice. (*J*) Average learning curves for learning of appropriate responses to CS+ and CS− were calculated based on the performance of control and CBPΔHAT^{PFC} groups across the entire training (Trial Blocks 1–6) (Fig. 1F,G) followed by fitting the regression line and t-test analysis on the mean of those slopes. The analysis of patterns of responses to CS+ and CS− in control animals tested on the context fear discriminatory task revealed that the improvement of fear memory accuracy was due to an incline in freezing to CS+ and a slight decline in freezing to CS− (CS+/Ctrl, $\alpha = 4.76 \pm 1.07$; CS−/Ctrl, $\alpha = -0.88 \pm 1.34$). The learning of appropriate responses to CS+ shows a positive slope (α) in both control and CBPΔHAT^{PFC} mice and there is no difference between groups (CS+/Ctrl, $\alpha = 4.76 \pm 1.07$; CS+/CBPΔHAT^{PFC}, $\alpha = 6.35 \pm 1.61$; CS+ slope/Ctrl vs. CBPΔHAT^{PFC} t-test, $t_{(18)} = -0.778$, $P = 0.446$). The CBPΔHAT^{PFC} group, which failed to improve fear memory accuracy, showed a positive slope for CS−, a marked difference from control responses to the CS− (CS−/Ctrl, $\alpha = -0.88 \pm 1.34$; CS−/CBPΔHAT^{PFC}, $\alpha = 4.26 \pm 1.4$); CS− slope/Ctrl vs. CBPΔHAT^{PFC} t-test, $t_{(18)} = -2.614$, $P = 0.018$). The asterisks indicate statistical significance: (*) $P < 0.05$, (**) $P < 0.01$, (n.s.) not significant.
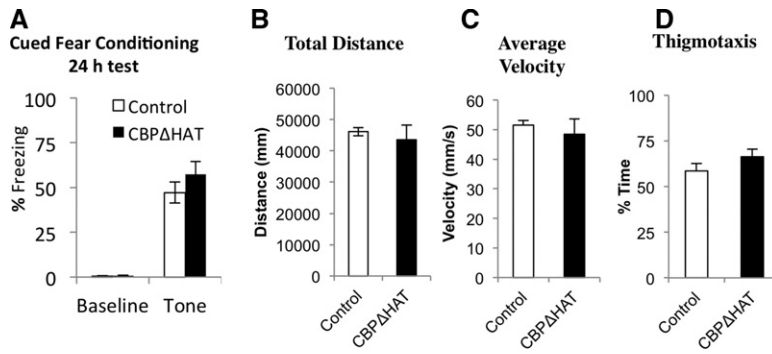
Figure 2. Pavlovian fear conditioning and locomotor activity are normal in CBPΔHAT^{PFC} mice. (*A*) Pavlovian cued fear conditioning was normal in CBPΔHAT^{PFC} mice. CBPΔHAT^{PFC} and control (Ctrl) mice showed normal acquisition and retention of contextual fear conditioning. Contextual fear was tested in context A at 24 h after the five CS–US pairing (CS, 2 sec, 2800-Hz tone; US, –foot shock). CBPΔHAT^{PFC} mice, $n = 10$. Control, $n = 10$. (*B*,*C*) Noninduced locomotor activity and (*D*) anxiety-related responses were unaltered in CBPΔHAT^{PFC} mice.

comparisons indicated that differences were present during Days 11 (CS+ vs. CS− *t*-test, $t_{(28)} = 3.149$, $P = 0.004$, $r = 0.51$) and 12 ($t_{(28)} = 3.325$, $P = 0.002$, $r = 0.53$) only. In contrast to the control animals, CBPΔHAT^{PFC} mice continued to generalize their conditioned responses after 2 d of training and failed to distinguish between context A and B during Days 9 and 10 (Day 9, $P = 0.286$; Day 10, $P = 0.291$).

Clearly, CBPΔHAT^{PFC} mice demonstrated a strong deficit in auditory memory specificity when compared to controls (RM-ANOVA of Group and FM-sweep direction and Days 7–12: Group × FM-sweep direction × Day, $F_{(2.8,81.4)} = 3.033$, $P = 0.037$; Group × FM-sweep direction, $F_{(1,29)} = 7.86$, $P = 0.009$; CBPΔHAT^{PFC}, $n = 15$; Ctrl, $n = 16$) (Fig. 4D,E). Furthermore, analysis of discrimination ratios shows a difference in performance between control and CBPΔHAT^{PFC} animals on Days 10–12 (Discrimination Index CBPΔHAT^{PFC} vs. Ctrl *t*-test: Day 10, $t_{(29)} = 2.813$, $P = 0.0087$, $r = 0.46$; Day 11, $t_{(29)} = 3.546$, $P = 0.001$, $r = 0.55$; Day 12, $t_{(29)} = 3.643$, $P = 0.001$, $r = 0.56$; CBPΔHAT^{PFC}, $n = 15$; Ctrl, $n = 16$) (Fig. 4G) but not during the initial phase of training. Clearly, control mice show better performance than CBPΔHAT^{PFC} mice on auditory discrimination (Fig. 4D,E,G). Taken together, these data demonstrate that CBPΔHAT expressed in the mPFC resulted in abnormal auditory (FM-sweep direction) fear memory specificity.

Similarly to CBPΔHAT^{PFC} animals, mCREB^{PFC} mice demonstrated a strong deficit in memory specificity during the discrimination phase when compared to controls on the auditory discrimination task (RM-ANOVA, Group × FM-sweep direction × Day: $F_{(2.8,79.6)} = 4.644$, $P = 0.006$; mCREB^{PFC}, $n = 14$; Ctrl, $n = 16$) (Fig. 4F). These data demonstrated that mCREB^{PFC} expressed in the mPFC prevented an improvement of auditory memory accuracy across the training as observed in control mice (Fig. 4D). Analysis of the auditory discrimination ratio confirmed that at the end of the training, the control animals performed better on the auditory discrimination task compared to the mCREB^{PFC} mice (RM-ANOVA of Day and Group: Day × Group, $F_{(2.5,69.0)} = 5.149$, $P = 0.005$; mCREB^{PFC}, $n = 14$; Ctrl, $n = 16$) (Fig. 4H). Furthermore, analysis of discrimination ratios showed a strong difference in performance between control and mCREB^{PFC} animals on Days 10–12 (*t*-test: Day 10, $t_{(28)} = 2.232$, $P = 0.034$, $r = 0.39$; Day 11, $t_{(28)} = 4.130$, $P = 0.0003$, $r = 0.62$; Day 12, $t_{(28)} = 4.313$, $P = 0.0002$, $r = 0.63$; mCREB^{PFC}, $n = 14$; Ctrl, $n = 16$).

Next, we performed an analysis of fear responses to upsweep (CS+) and, separately, to downsweep (CS−) in control, CBPΔHAT^{PFC}, and mCREB^{PFC} mice tested on FM-sweep direc-

tion fear discriminatory task (Fig. 4). There was no difference in responses to conditioned stimuli CS+ between CBPΔHAT^{PFC} and control mice across the entire FM-sweep direction discrimination training (CS+/CBPΔHAT^{PFC} vs. Ctrl: RM-ANOVA of Days 7–12 and group, Day × Group, $F_{(2.8,81.6)} = 0.756$, $P = 0.514$) (Fig. 4D,E). Similarly, there was no difference in responses to conditioned stimuli CS+ between mCREB^{PFC} and control mice across the entire FM-sweep direction discrimination training (CS+/mCREB^{PFC} vs. Ctrl: RM-ANOVA of Days 7–12 and group, Day × Group, $F_{(2.8,79.5)} = 1.808$, $P = 0.155$) (Fig. 4D,F). An analysis of learning curves (Fig. 4J) showed a positive slope to CS+ in control ($\alpha = 2.366 \pm 0.82$) and CBPΔHAT^{PFC} ($\alpha = 2.384 \pm 0.894$) mice or no change in freezing responses to CS+ in mCREB^{PFC} mice ($\alpha = -0.278 \pm 1.15$) across the entire FM-sweep direction fear discriminatory task. In fact, there was no difference in the learning (slopes) of appropriate responses to CS+ between CBPΔHAT^{PFC} and control groups (CS+ slope/Ctrl vs. CBPΔHAT^{PFC} *t*-test, $t_{(29)} = -0.015$, $P = 0.988$) (Fig. 4J) or mCREB^{PFC} and control mice (CS+ slope/Ctrl vs. mCREB^{PFC} *t*-test, $t_{(28)} = 1.906$, $P = 0.067$) (Fig. 4J). However, CBPΔHAT^{PFC} and mCREB^{PFC} mice responded differently to nonrelevant stimuli CS− across training on the auditory discriminatory task when compared to normal mice (CS−/CBPΔHAT^{PFC} vs. Ctrl, RM-ANOVA of Days 1–5 and group, Day × Group, $F_{(3.8,111.4)} = 6.151$, $P = 0.0002$; CS−/mCREB^{PFC} vs. Ctrl, RM-ANOVA of Days 1–5 and group, Day × Group, $F_{(3.7,103.8)} = 5.685$, $P = 0.0005$) (Fig. 4D,E). When compared to control mice, change in freezing (freezing Δ) to CS− across the training was also significantly different in CBPΔHAT^{PFC} (*t*-test, $t_{(29)} = -2.798$, $P = 0.009$) (Fig. 4I) and in mCREB^{PFC} mice (*t*-test, $t_{(28)} = -2.466$, $P = 0.02$) (Fig. 4I). The marked improvement of discrimination observed on the FM-sweep direction fear discriminatory task in control mice
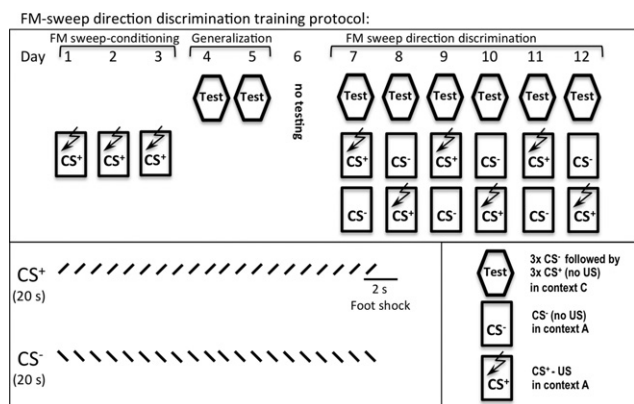

Figure 3. Experimental design for the auditory discrimination test. The auditory discrimination task tests the ability of subjects to recognize a direction of FM-sweeps (trains of upward and downward FM-sweeps). The conditioned stimuli (CS) for auditory fear conditioning were 20-sec trains of FM-sweeps for a 400-msec duration, logarithmically modulated between 2 and 13 kHz (upsweep) or 13 and 2 kHz (downsweep) delivered at 1 Hz at 75 dB. As described in Materials and Methods, these assays include three phases: FM-sweep conditioning (Days 1–3), generalization (Days 4–5), and FM-sweep direction discrimination training (Days 6–12).

(Fig. 4D,G,J) coincides with the significant negative slope of the learning curve for CS− ($\alpha = -6.176 \pm 1.22$) (Fig. 4J). The CBPΔHAT[PFC] group, which failed to improve fear memory accuracy across training (Fig. 4E,G), shows only a slight negative slope for CS− across the training ($\alpha = -1.22 \pm 0.78$) (Fig. 4J) and a marked difference when compared to the CS− slope observed in control animals (CS− slope/Ctrl vs. CBPΔHAT[PFC] t-test, $t_{(29)} = -3.368$, $P = 0.002$) (Fig. 4J). The mCREB[PFC] group, which did not improve performance on the auditory discrimination task as well (Fig. 4F,H), exhibited similar patterns of learning to the CBPΔHAT[PFC] mice. While responses to CS+ do not vary from those observed for control mice (Fig. 4I,J), the CS− learning curve is significantly different in mCREB[PFC] mice compared to control mice (CS−/Ctrl, $\alpha = -6.176 \pm 1.22$; CS−/mCREB[PFC], $\alpha = -0.746 \pm 1.03$; CS− slope/Ctrl vs. mCREB[PFC] t-test, $t_{(28)} = -3.347$, $P = 0.002$) (Fig. 4J).

In summary, analysis of patterns of responses to CS+ and CS− in control animals tested on the FM-sweep direction fear discriminatory task revealed that the improvement of auditory fear memory accuracy was due to only a slight incline in freezing to CS+ and rapid decline in freezing to CS−. CBP hypofunction or CREB hypofunction in the mPFC altered the ability to learn auditory discriminatory responses to CS+ vs. CS− by disrupting the pattern of learning for CS− only, while responses to CS+ remained similar to those of control mice. Consistent with conclusions regarding contextual fear memory specificity, these data demonstrate that the mPFC supports the improvement of auditory fear memory accuracy by controlling acquisition of appropriate responses to nonrelevant stimuli.

Discussion

The present findings are the first evidence of the critical role that the mPFC plays in the attainment of fear memory accuracy for appropriate discriminative responses to aversive and nonaversive stimuli. They add substantially to the understanding of the circuitry and molecular mechanisms underlying fear memory specificity and generalization. We demonstrated that CBP-dependent signaling in the mPFC is required for fear memory accuracy. In addition, fear memory accuracy was also abnormal in mutant mice with disrupted CREB function, which is one of the most widely studied mediators of cellular memory consolidation in *Drosophila*, *Aplysia*, and mice (Dash et al. 1990; Bourtchuladze et al. 1994; Yin et al. 1994; Josselyn et al. 2001; Kida et al. 2002; Pittenger et al. 2002). The requirement of CBP acetyltransferase activity for memory consolidation has been demonstrated before, including acetylation/deacetylation-targeted pharmacological rescue of memory consolidation in CBPΔHAT mutant mice (Alarcon et al. 2004; Korzus et al. 2004) or late-phase LTP in CBP deficient mutant mice (Alarcon et al. 2004), and also in *Aplysia* (Guan et al. 2002).

It is important to note that Pavlovian auditory and contextual fear conditioning were intact in CBPΔHAT[PFC] and mCREB[PFC] mice. Memory generalization measured immediately after initial fear conditioning was also unchanged in CBPΔHAT[PFC] and mCREB[PFC] mice. In addition, there was no difference between tested groups in responses to CS+ across the entire contextual or auditory discriminatory tasks. The abnormal performance of mutant mice in contextual and auditory discriminatory tasks was specific to deficits in responsiveness to CS− only and during later phases of the tasks. These data suggest that the prefrontal circuit is critically involved in learning appropriate responses to nonrelevant stimuli that are similar yet not identical to aversive stimuli. These data are consistent with the previously described function of the PFC in fear memory extinction. Increasing evidence from human (Kesner and Rogers 2004; Blumenfeld and Ranganath 2007) and animal (Hirsch and Crepel 1992; Morris et al. 1999; Takita et al. 1999; Quirk et al. 2000; Izaki et al. 2002; Maroun and Richter-Levin 2003; Santini et al. 2004; Kawashima et al. 2006; Richter-Levin and Maroun 2010) studies implicate the PFC in extinction of conditioned fear (Sotres-Bayon et al. 2006; Quirk and Mueller 2008) and conditioned taste aversion (Akirav et al. 2006).
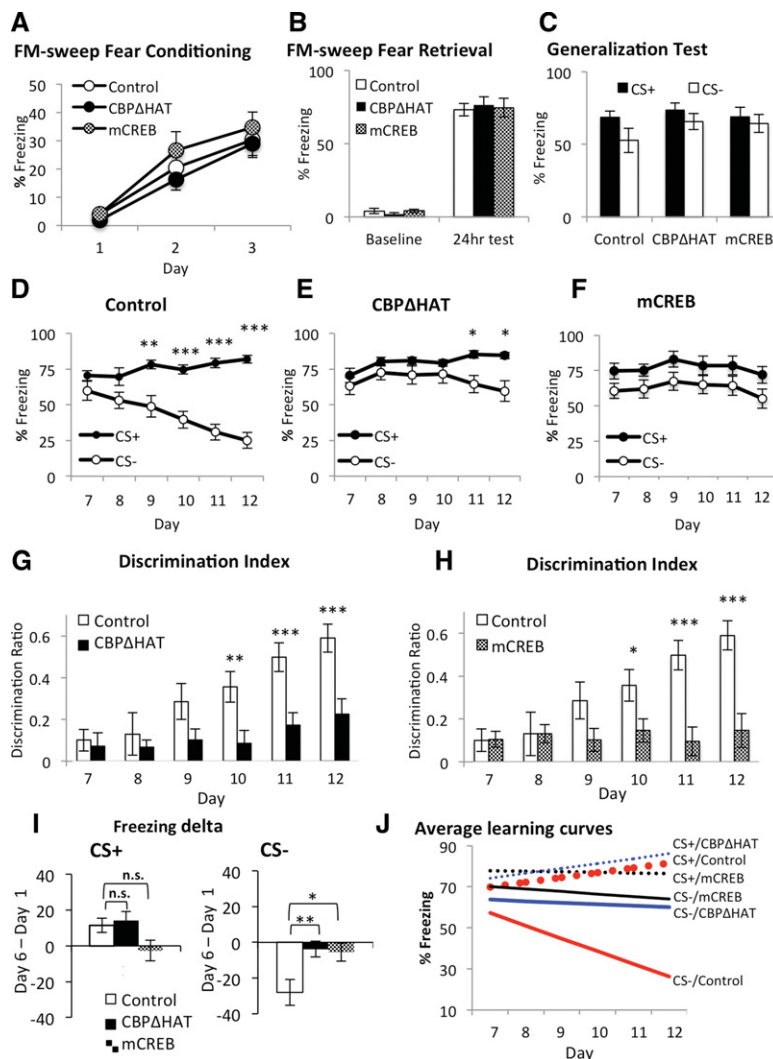

Figure 4. (Legend on next page)

There is converging evidence that links fear memory specificity and generality with information processing in the hippocampus–thalamus–PFC–amygdala circuit (Marr 1971; O'Reilly and McClelland 1994; Leutgeb et al. 2007; McHugh et al. 2007; Kumaran and McClelland 2012; Nakashiba et al. 2012; Xu et al. 2012; Navawongse and Eichenbaum 2013; Xu and Sudhof 2013). Involvement of the PFC in context or odor discrimination during information acquisition has been previously studied (DeVito et al. 2010; Xu et al. 2012; Xu and Sudhof 2013); however, the contribution of the PFC in the discrimination of auditory patterns, such as FM-sweep direction, has not been previously explored. FM-sweep direction discrimination is important in speech recognition (Zeng et al. 2005) but its underlying neural mechanism is unknown. Auditory fear conditioning has been extensively studied and depends on synaptic plasticity within the amygdala (Fanselow and LeDoux 1999; LeDoux 2000) but neural substrates for auditory fear discrimination are less well studied in mice. Recently, it was suggested that stimulus convergence in the auditory cortex is necessary for the associative fear learning of frequency-modulated sweeps (Letzkus et al. 2011). A reduced reliance on FM-sweep direction stimuli in CBPΔHAT^{PFC} and mCREB^{PFC} mice indicates that the mPFC supports directly auditory fear memory specificity.

There is a general difference in the patterns of freezing responses to CS+/CS− between auditory and context discrimination in control animals. While the direction of learning curves (upward/downward) remains the same, their steepness varies. In the context discrimination assay (Fig. 1J), the learning of appropriate responses to CS+ showed a significantly positive slope (CS+/Control, α = 4.76 ± 1.07, where α = slope) (Fig. 1J), while the learning of the appropriate response to CS− showed a slight negative slope (CS−/Control, α = −0.88 ± 1.34) (Fig. 1J). The marked improvement of discrimination observed on the FM-sweep direction fear discriminatory task in control mice (Fig. 4D) coincides with the slight positive slope of the learning curve for CS+ (CS+/Control, α = 2.366 ± 0.82) (Fig. 1J) and the significant negative slope of the learning curve for CS− (CS−/Control, α = −6.176 ± 1.22) (Fig. 1J). Two possible factors may have an effect on the steepness of learning curves for acquired responses to CS+/CS− in these discriminatory tasks. First, it is possible that a "floor" effect on CS− curve in the contextual discriminatory task and a "ceiling" effect on CS+ curve in the auditory discriminatory task may account for these differences. The initial level of freezing is substantially lower in the contextual discriminatory task (∼25% of initial freezing) (Fig. 1F,G) when compared to the auditory discrimination task (>75% of initial freezing) (Fig. 4D–F). Second, it may be more difficult to extinguish responses to nonrelevant stimuli (Context B) because of the high complexity of contextual stimuli (multimodality, more details). Conversely, the rapid decline of responses to downsweep (CS−) may result from the lower complexity (single modality) of the auditory stimuli and, subsequently, more effective discrimination training.

Recently, it has been proposed that disruption of the PFC circuit during information acquisition may result in overgenerality. Inactivation of prefrontal inputs to the nucleus reuniens resulted in an increased fear generalization to novel contextual stimuli (Xu et al. 2012). Our manipulation of the mPFC differed and targeted CBP-dependent nuclear processes, which may not produce immediate global effects on firing properties of the mPFC neurons during information acquisition, but rather have effects on the properties of the neural circuits relevant to long-term memory consolidation. However, it is unclear whether the abnormality in fear memory accuracy found in CBPΔHAT^{PFC} mice resulted from fear driven overgeneralization or a deficit to access memory details (i.e., memory resolution).

The difficulties with studying CBP function in cognition are confounded by the high complexity of the CBP protein, which can integrate or antagonize multiple signaling pathways, and by its distinctive roles in developing and mature circuits. Haploid insufficiency mutations in CBP (Chrivia et al. 1993) or its homolog p300 (Eckner et al. 1994) result in Rubinstein–Taybi syndrome (RTS) (Rubinstein and Taybi 1963; Petrij et al. 1995), which is a developmental disorder characterized by severe mental retardation. CBP and p300 both share a very similar molecular structure (Arany et al. 1994), including intrinsic acetyltransferase activity (Ogryzko et al. 1996), and are capable to mediate similar cellular functions including CREB-dependent transcriptional activation. The functional differences between these two redundant genes are due to their highly overlapping but different patterns of expression and not yet understood

Figure 4. FM-sweep direction fear memory specificity is deficient in CBPΔHAT^{PFC} mice. (*A,B*) Pavlovian FM-sweep fear conditioning was normal in CBPΔHAT^{PFC} and mCREB^{PFC} mice. CBPΔHAT^{PFC} and mCREB^{PFC} mice showed similar acquisition (*A*) and retention (*B*) of FM-sweep fear conditioning to control (Ctrl) mice. FM-sweep fear was tested in context C at 24 h after a three upsweep–foot shock pairing. (*C*) All three groups (CBPΔHAT^{PFC} and mCREB^{PFC} and Ctrl) show no difference in the freezing responses to CS+ and CS− (*P* > 0.05) during Days 4 and 5 of training, indicating that, initially, the CBPΔHAT^{PFC} and mCREB^{PFC} mice generalized responses and did not discriminate between upsweep and downsweep. (*D*) After the initial generalization of fear conditioned responses, control mice exhibited robust fear memory specificity. (*E*) CBPΔHAT^{PFC} mice did not discriminate between upsweep and downsweep and exhibited a deficit in auditory fear memory specificity. CBPΔHAT^{PFC} mice demonstrated strong deficit in auditory memory specificity when compared to controls (RM-ANOVA, Treatment × Context × Trial Blocks 1–6, $F_{(2.806,81.366)}$ = 3.033, *P* = 0.037) (Fig. 1B,C). (*F*) Similarly to CBPΔHAT^{PFC}, mCREB^{PFC} mice did not discriminate between upsweep and downsweep and exhibited a deficit in auditory fear memory specificity. (*G*) The FM-sweep direction discrimination ratios (DI) were calculated using the freezing responses to CS+ and CS− according to the formula DI = ([Upsweep − Downsweep]/[Upsweep + Downsweep]). Analyses revealed differences between CBPΔHAT^{PFC} and control mice in the performance during Days 11–12 between CBPΔHAT^{PFC} and control mice. CBPΔHAT^{PFC}, *n* = 15; Ctrl, *n* = 16. (*H*) Analyses revealed differences between mCREB^{PFC} and control mice in the performance during Days 11–12. mCREB^{PFC}, *n* = 14; Ctrl, *n* = 16. (*I*) Change in freezing across training (freezing Δ), calculated as the (freezing on Day 12 − freezing on Day 7). There was no difference in responses to conditioned stimuli CS+ between CBPΔHAT^{PFC}, mCREB^{PFC}, and control mice. Change in freezing to CS− across the training was significantly higher in CBPΔHAT^{PFC} and mCREB^{PFC} when compared to control mice. (*J*) Average learning curves for learning of appropriate responses to CS+ and CS− were calculated based on the performance of control and CBPΔHAT^{PFC} group across the entire training (*D–F*), Days 7–14, followed by fitting the regression line and *t*-test analysis on the mean of those slopes (α). The analysis of patterns of responses to CS+ and CS− in control animals tested on the FM-sweep direction fear discriminatory task revealed that the improvement of auditory fear memory accuracy was due to a slight incline in freezing to CS+ and rapid decline in freezing to CS− (CS+/Ctrl, α = 2.366 ± 0.82; CS−/Ctrl, α = −6.176 ± 1.22). There was no difference in the learning (slopes) of appropriate responses to CS+ between CBPΔHAT^{PFC} and control groups (CS+/Ctrl, α = 2.366 ± 0.82; CS+/CBPΔHAT^{PFC}, α = 2.384 ± 0.894; CS+ slope/Ctrl vs. CBPΔHAT^{PFC} *t*-test, $t_{(29)}$ = −0.015, *P* = 0.988) or mCREB^{PFC} and control mice (CS+/Ctrl, α = 2.366 ± 0.82; CS+/mCREB^{PFC}, α = −0.278 ± 1.15; CS+ slope/Ctrl vs. mCREB^{PFC} *t*-test, $t_{(28)}$ = 1.906, *P* = 0.067). The CBPΔHAT^{PFC} group, which failed to improve fear memory accuracy, showed a positive slope for CS−, a marked difference from control responses to the CS− (CS−/Ctrl, α = −6.176 ± 1.22; CS−/CBPΔHAT^{PFC}, α = −1.22 ± 0.78; CS− slope/Ctrl vs. CBPΔHAT^{PFC} *t*-test, $t_{(29)}$ = −3.368, *P* = 0.002). Similar to the CBPΔHAT^{PFC} group, the mCREB^{PFC} group did not improve performance on the auditory discrimination task and showed a positive slope for CS−, a marked difference from control responses to the CS− (CS−/Ctrl, α = −6.176 ± 1.22; CS−/mCREB^{PFC}, α = −0.746 ± 1.03; CS− slope/Ctrl vs. mCREB^{PFC} *t*-test, $t_{(28)}$ = −3.347, *P* = 0.002). The asterisks indicate statistical significance: (*) *P* < 0.05, (**) *P* < 0.01, (***) *P* < 0.001, (n.s.) not significant.

functional specificity. Prenatal lethality in CBP knockout mice demonstrates an essential role of this gene in embryogenesis (Yao et al. 1998). CBP hemizygote or CBP mutations targeted to excitatory forebrain neurons using CamKIIα promoter driven expression, such as conditional knockout or transgenic mice expressing dominant negative variants, display specific deficits in long-term memory but not in short-term memory suggesting that CBP function may support long-term memory encoding. However, these results are not consistent across all CBP mutant strains. In one study, CamKIIα-dependent conditional knockout of CBP targeted to excitatory neurons during postnatal brain development resulted in deficient short-term memory (Chen et al. 2010). Although CamKIIα gene product levels are low during early phases of brain development, a large increase in the expression is usually observed between postnatal days 10 to 30 (Sugiura and Yamauchi 1992; Kojima et al. 1997) coinciding with postnatal brain development. Since the developmental time of CBP conditional deletion was not reported in this study, one cannot eliminate developmental confounds underlying the behavioral phenotype. Thus, it is difficult to dissociate between developmental defects, developmental compensatory effects, and acute deficits in mutant mice with CBP hypofunction during critical periods of postnatal brain development. However, when manipulation of CBP activity is performed in the adult brain, data consistently implicate CBP acetyltransferase function in neural epigenetic signaling underlying long-term synaptic plasticity and long-term memory consolidation (Korzus et al. 2004; Barrett et al. 2011; Maddox et al. 2013). In addition, testing of CamKIIα positive cell-restricted and adult mice induced CBP knockout mice indicated that environment-induced adult neurogenesis is extrinsically regulated by CBP function in mature hippocampal granule cells (Lopez-Atalaya et al. 2011). Considering that adult neurogenesis in the hippocampus constitutes an adaptive mechanism to optimally encode contextual information important for memory resolution (Aimone et al. 2011; Sahay et al. 2011) and CBP mutant demonstrates deficiency in spatial discrimination (Lopez-Atalaya et al. 2011) it is likely that CBP is also involved in adult neurogenesis-dependent long-term encoding of contextual information. However, in CBPΔHAT^{PFC} or mCREB^{PFC} mice hypofunction was targeted to the mPFC and it is unlikely that this manipulation would have an effect on adult neurogenesis in the hippocampus.

How can CBP enzymatic activity regulate neural function? The regulation of gene expression requires not only an activation of transcription factors but also the recruitment of multifunctional coactivators that are independently regulated and directly involved in the chromatin remodeling underlying epigenetic regulatory mechanisms (Rosenfeld and Glass 2001). For example, recent work demonstrated the importance of chromatin remodeling factors like the SWI/SNF complex in neuronal function underlying memory (Vogel-Ciernia et al. 2013). While CBP's function as a platform to recruit other required coactivators appears to be indispensable for CREB-dependent transcription, the recruitment for lysine acetyltransferase activity is transcription unit specific and may depend on the structure of chromatin at a specific locus and/or a specific cell type (Puri et al. 1997; Korzus et al. 1998). Changes in histone acetylation are predictive for gene expression (Allfrey et al. 1964; Pogo et al. 1966). The concordance between the histone acetylation and transcription levels increases over time and the positive correlation between both has been confirmed in genome-wide studies (Kurdistani and Grunstein 2003; Karlic et al. 2010; Markowetz et al. 2010). It is important to emphasize that these are correlations only and that causal relationships between histone modification and gene expression in the brain in vivo will require additional investigation. In addition, a number of nonhistone proteins have been identified as substrates

for CBP (Kouzarides 2000; Sterner and Berger 2000; Yang 2004; Glozak et al. 2005; Kimura et al. 2005) including CREB (Lu et al. 2003). Regardless of the uncertainty of the CBP's acetyltransferase critical target(s), genetic and pharmacological studies have indicated that hypofunction of CBP's acetyltransferase activity interferes with mechanisms that support memory consolidation and reconsolidation in brain neural networks (Korzus et al. 2004; Maddox et al. 2013). Current data indicate that the acquisition fear memory accuracy involves CBP-dependent mechanism within mPFC circuitry.

Thus, locomotor activity, anxiety-related responses, and fear conditioning were normal in CBPΔHAT^{PFC} mice, yet these mutant mice showed a strong deficit in fear memory accuracy in both contextual and auditory discrimination assays. Both context and auditory fear discrimination tasks required temporal integration because the animals learned subtle differences between relevant and nonrelevant stimuli over many days with a single exposure to both CS+ and CS− per day. Inhibition of a component of neural signaling immediately upstream of CBP by a direct blockade of CREB ability to recruit CBP to the target promoter in the mPFC produced identical effects as CBPΔHAT on the capability of mice to learn the distinction between auditory stimuli. Thus, impairment of either component of CREB/CBP-dependent signaling (CREB phosphorylation or CBP's acetyltransferase activity) within the mPFC circuitry resulted in a deficit in auditory fear memory specificity indicating that the mPFC circuitry supports the disambiguation of auditory fear signals.

How CBP and CREB control memory accuracy in the mPFC is unclear. Both CBP and especially CREB have been implicated in long-term plasticity and memory consolidation in *Aplysia*, *Drosophila*, and mice. Thus it is possible that long-term coding within mPFC network involving LTP-mediated modification of prefrontal circuits is critical during contextual and auditory fear discrimination. This type of plasticity in the mPFC might be required to extinguish CS− responses, which would be consistent with the recognized role of the mPFC in fear memory extinction. In addition, CREB has been strongly implicated in adaptive alteration of neuronal excitability and memory allocation (Rogerson et al. 2014) and it is possible that CBP may mediate CREB-dependent changes in neuronal excitability.

There is converging evidence that links contextual fear memory specificity and generality with information processing in the hippocampus–thalamus–PFC–amygdala circuit (Marr 1971; O'Reilly and McClelland 1994; Leutgeb et al. 2007; McHugh et al. 2007; Kumaran and McClelland 2012; Nakashiba et al. 2012; Xu et al. 2012; Navawongse and Eichenbaum 2013; Xu and Sudhof 2013). Our findings are consistent with the conclusions reported by DeVito et al. (2010), who suggested that the mPFC circuit was critical for the acquisition of overlapping odor discrimination problems. Thus, the present findings of the critical role of the mPFC in auditory and context discrimination provide further evidence for the high integration-dependent disambiguation function of the mPFC because similar contexts (or up/down FM-sweeps) were both presented during multiple day training consisting of discontiguous episodes before the animals acquired the ability to properly respond to these signals. These data indicate that certain types of prefrontal dysfunction are likely to contribute to overgeneralized fear, a clinical condition present in anxiety related disorders such as PTSD.

Materials and Methods

Subjects

C57BL/6J mice were used for all experiments. Prior to any procedure, the mice are weaned at postnatal day 21, housed four

animals to a cage with same-sex littermates, maintained on a 12-h light–dark cycle, and had ad libitum access to food and water. Autoclaved bedding was changed every week. All procedures were approved by the UC Riverside Institutional Animal Care and Use Committee in accordance with the NIH guidelines for the care and use of laboratory mice.

Surgery

The injection protocol has been previously described by Cetin et al. (2006). In this study, 2- to 4-mo-old mice were individually housed and weighed to determine the appropriate drug ratios to use. Atropine was injected to help with breathing (0.02 mg/kg body weight). The mice were then placed into an isoflurane chamber to induce anesthesia, mounted in a heated stereotaxic apparatus, and supplied with a constant flow of isoflurane/oxygen mix. The scalp was shaved and sanitized with 70% ethanol. The ear bars, bite bar, and nose clamp were adjusted to firmly hold the head in place. A midline incision was made on the scalp, and surgical hooks were placed to keep the skull exposed. Sterile PBS was added as needed to prevent the skull from drying. The head was leveled by comparing bregma and lambda coordinates until they were equivalent. Injection sites were calculated based on bregma coordinates, and a dental drill was used to thin the skull over the injection site. A 27G needle was then used to remove the thinned bone. A 5-µL calibrated glass micropipette (8-mm taper, 8-µm internal tip diameter) was fitted with a plastic tube connected to a 10-mL syringe and lowered onto a square of Parafilm containing a 4-µL drop of virus. The syringe was aspirated to fill the micropipette with solution before moving it to the injection site. The micropipette was slowly lowered to the proper stereotaxic coordinates and pressure was applied to the syringe to inject 1 µL of solution at a rate of 50 nL/min. After the total volume was injected, the micropipette was withdrawn slowly to avoid backflow, and the injection site was cleaned with sterile cotton swabs. The skin was sutured, and antibiotic was applied to the scalp. Lidocaine was subcutaneously injected near the site followed by an intraperitoneal injection of sterile PBS (30 mL/kg body weight) to prevent dehydration. The mouse was kept warm by placing its cage on a heated plate and injected with buprenorphine (0.05 mg/kg) for pain relief. On post-surgical Days 1 and 2, the mouse received subcutaneous injections of meloxicam (1 mg/kg) to relieve pain. Animals were monitored for any signs of distress or inflammation for 3 d after surgery. Behavioral experiments were initiated 3 d after surgery. The infralimbic and prelimbic cortices were targeted at the following stereotaxic coordinates: bregma, AP 1.8, ML ± 0.4, DV 1.4.

Viruses

Surgical procedures were standardized to minimize the variability of HSV virus injections, using the same stereotaxic coordinates for the mPFC and the same amount of HSV injected into the mPFC for all mice. CBPΔHAT or mCREB and/or EGFP were cloned into the HSV amplicon and packaged using a replication-defective helper virus as previously described (Lim and Neve 2001; Neve and Lim 2001). The viruses (HSV/CMV-CBPΔHAT-IRES2-EGFP, HSV/CMV-EGFP, and HSV/mCREB-EGFP) were prepared by Dr. Rachael Neve (MIT, Viral Core Facility). The average titer of the recombinant virus stocks was typically 4.0×10^7 infectious units/mL. HSV viruses are effectively expressed in neurons in the PFC. The CBPΔHAT mutant, a dominant-negative inhibitor of CBP-dependent histone acetylation, harbors a substitution mutation of two conserved residues (Tyr^{1540}/Phe^{1541} to Ala^{1540}/Ala^{1541}) in the acetyl CoA binding domain (Korzus et al. 1998). It has been also demonstrated that CBPΔHAT lacks histone acetyltransferase activity (Korzus et al. 2004) and blocks c-fos expression in neurons (Korzus et al. 2004). The dominant negative CREB mutant (mCREB) carries substitution mutation Ser^{133} to Ala^{133}. Previous studies indicate that mCREB decreased CREB function and blocked neuronal CREB dependent gene expression (Gonzalez et al. 1989; Chrivia et al. 1993; Barrot et al. 2002; Olson et al. 2005).

Behavioral assays

All behavioral experiments were performed under blind conditions.

Fear conditioning

Fear conditioning was performed as previously described (Korzus et al. 2004). Fear conditioning training was performed in the fear conditioning box from Coulburn Instruments Inc. After being handled, individual mice were exposed to context A. Context A was the unmodified fear conditioning box, which was placed inside a sound attenuated chamber with the house light and house fan turned on. Performance was scored by measuring freezing behavior, the complete absence of movement (Fanselow 1980). Freezing was scored and analyzed automatically by a Video-based system (Freeze Frame software ActiMetrics Inc.). Video was recorded at 30 frames/sec. The Freeze Frame software calculated a difference between consecutive frames by comparing gray scale value for each pixel in frame. Freezing was defined based on experimenter observations and set as subthreshold activity for longer than 1 sec. Freezing was expressed as a % Freezing, which was calculated as a percent of freezing time per total time spent in the testing chamber. The chamber was cleaned in between trials with Quatricide, 70% ethanol, and distilled water.

Contextual fear conditioning. Mice were trained in a standard fear conditioning chamber (Coulburn Instruments Inc.). The individual mice were exposed to context A for 180 sec and received a 0.75-mA, 2-sec foot shock (context A–foot shock pairing). The animals were then left for another 180 sec inside the chamber. For the memory retention test, the mice were placed back into the training chamber for 180 sec. Freezing was scored and analyzed automatically as described above.

Cued fear conditioning. Mice were trained in a standard fear conditioning chamber (Coulburn Instruments Inc.). After a 3-min baseline period, one, two, or three 20-sec tones (2800 Hz, 75 dB) were played and a shock (0.75 mA, 2 sec) was delivered during the final 2 sec of the tone. Twenty-four hours later, mice were placed in a novel enclosure and, after a 3-min baseline exposure, a series of three tones identical to that given in the training session was played. Freezing was scored and analyzed automatically as described above.

Context discrimination. The context discrimination assay was preformed similarly as previously described (Lovelace et al. 2014). After being handled, individual mice were exposed to context A 1 d before training. The protocol included 14 d of training, which was divided into three phases: initial training phase, generalization test, and discrimination phase (Fig. 1D). During the initial training phase (Day 1), mice were placed in the context A for 180 sec followed by a single foot shock (arrow) and left for another 60 sec inside the chamber. Context A (CS+) was the unmodified fear conditioning box (Coulburn Instruments Inc.), which was placed inside a sound attenuated chamber with the house light and house fan on. The chamber was cleaned with Quatricide, 70% ethanol, and distilled water. For generalization test and during discrimination phase, the individual mice were exposed to Context A for 180 sec and received a 0.75-mA, 2-sec foot shock, and left for another 60 sec inside the chamber. Four hours later, the mice were exposed to the similar Context B (CS−) for 242 sec and received no foot shock. Context A and B were similar but not the same. Context B was the modified fear conditioning chamber, with angular wall inserts, house fan off, and scented with Simple Green. Thus animals were exposed to CS+ 13 times before the final test. The order of exposure to different contexts was counter balanced. Additionally, the context cues themselves were counter balanced within each group in order to isolate the effect of the CS+.

Auditory discrimination. The auditory discrimination task is divided into three phases: initial training phase, generalization test, and

discrimination phase (Fig. 3). The conditioned stimuli (CS) for auditory fear conditioning were 20-sec trains of frequency modulated (FM)-sweeps for a 400-msec duration, logarithmically modulated between 2 and 13 kHz (upsweep) or 13 and 2 kHz (downsweep) delivered at 1 Hz at 75 dB. After habituation, the CS+ was paired with a foot shock (2 sec, 0.75 mA). The onset of the US coincided with the onset of the last sweep for the CS. For fear conditioning acquisition (Days 1–3; initial training phase), the animals were presented with a single US–CS pairing per day. The FM-sweep Fear Retrieval (Day 4) and Generalization (Days 4–5) were tested (freezing to 3 × CS− for 30 sec followed by 3 × 30-sec CS+ without US; 3-min baseline and 3-min ITI) in context C, which significantly differed from the training chamber (context A). The discrimination phase of FM-sweep direction discrimination training was performed over three sessions a day for 6 d (Days 7–12): Session 1 was the performance test, Session 2 was the presentation to 1 × UC–CS+ pairing after a 3-min baseline, and Session 3 was the presentation to the US–CS− pairing after a 3-min baseline. The CS+ and CS− were counterbalanced such that half of the CS+ group was upsweep and the other half of CS+ was downsweep.

Open–field test. A 17″ × 17″ × 12″ clear Plexiglas arena with a white acrylic floor was used for the open-field test. The arena was placed in a sound attenuated chamber with a ceiling mounted camera and a dim light. After sanitizing the arena with Quatricide, 70% EtOH, and distilled water, the mice were individually placed inside the chamber and allowed to explore for 15 min before being returned to their home cage. Videos are analyzed offline using behavioral analysis software (CleverSys, Inc.) to quantify the level of anxiety and locomotion.

Histology

Mice were anesthetized using Nembutal (200 mg/kg, i.p. injection) and transcardially perfused first with PBS and then 4% PFA. The extracted brain was soaked in 4% PFA overnight and then transferred to PBS until histological sectioning. In this study, 100-μm-thick sections of the mPFC were obtained using a Compresstome VF-300 (Precisionary Instr.) and placed in a 24-well plate for free-floating immunohistochemistry (IHC) according to a previously described protocol (Korzus et al. 2004). The sections are washed three times for 10 min in a wash buffer (PBS, 0.3% Triton X-100, 0.02% NaN₂) followed by a 1-h incubation in blocking buffer (5% normal goat serum in washing buffer), followed by a 10-min incubation in the wash buffer. The sections were incubated overnight at 4C° with primary antibodies: anti-NeuN (Millipore, 1:2000), chicken anti-GFP (Molecular Probes, 1:1000), anti-acetyl-Histone H3 (Millipore, 1:2000), or anti-acetyl-Histone H4 (Millipore, 1:2000). After three washes with the wash buffer, the sections were incubated with secondary antibodies (Alexa647-goat anti-mouse IgG, Alexa488-goat anti-chicken IgG, Alexa647-goat anti-rabbit IgG; Molecular Probes, 1:1000), in blocking buffer for 4 h at room temperature. The sections were washed again three times with the wash buffer before mounting for viewing. Negative control slices were performed for each row of the well plate, undergoing the same IHC procedure in addition to receiving primary antibodies. After immunostaining, the tissue was mounted directly onto glass slides, covered, and sealed with nail polish before imaging.

Imaging

The slides were placed on the stage of an Olympus FV1000 laser scanning confocal microscope controlled using the FluoView software. GFP and Alexa-647 were imaged using 473-nm and 647-nm lasers, respectively. The background fluorescence was measured and subtracted for each image. The fluorescence intensity was compared to the negative control slices, which did not receive any primary antibodies. Immunostained tissue was analyzed using a semiautomatic laser scanning confocal microscope (Olympus FV1000) controlled by the FluoView software. Multiple brain sections were imaged using identical microscope

settings. Eighty-micrometer z-stacks were obtained from the PL region in the mPFC, and region of interest (ROI) analysis was used for quantification. The background fluorescence was measured for each image and then subtracted. The intensity quantification was performed using the FluoView Olympus software and NIH Image J.

Histone acetylation assay

Individual mice were trained on a fear conditioning paradigm in which they were presented with a 20-sec auditory stimulus followed immediately by a 2-sec foot shock (0.75-mA intensity). The auditory stimulus is the same as used for behavioral training in which logarithmically modulated upward (2–13 kHz) frequency-modulated sweeps are presented in 400-msec bouts at a 1-Hz frequency for a total duration of 20 sec. Three minutes after the foot shock, mice were placed in their home cage for 25 min undisturbed. Immunohistology and imaging were performed as described above. The region of interest (ROI) was a 5-μm circle placed on cells expressing GFP within cortical layer 2/3 in mPFC and fluorescence corresponding to acetylated histone H3 or H4 was measured from randomly selected 50–60 cells per hemisphere. The fluorescence intensity quantification was performed on original images by the use of Olympus Fluoview software.

Data analysis

The experimenters were blind to the group conditions. Data are expressed as the means ± SEM. *N* indicates number of animals unless stated otherwise. Statistical analysis was performed using Excel (Microsoft Inc.) or SPSS (IBM Inc.). The Student's *t*-test or ANOVA was used for statistical comparisons. Pearson's correlation (*r*) was used as an effect size. In cases where the repeated measures ANOVA (RM-ANOVA) was utilized and assumptions of sphericity were violated (via Mauchly's Test), the analysis was performed using the Greenhouse–Geisser correction. Where applicable, post hoc analysis with Bonferroni correction was performed for multiple comparisons, which allows for substantially conservative control of the error rate. A $P < 0.05$ was considered statistically significant. The asterisks indicate statistical significance: (*) $P < 0.05$, (**) $P < 0.01$, (***) $P < 0.001$, (n.s.) not significant.

References

Aimone JB, Deng W, Gage FH. 2011. Resolving new memories: a critical look at the dentate gyrus, adult neurogenesis, and pattern separation. *Neuron* **70:** 589–596.

Akirav I, Khatsrinov V, Vouimba RM, Merhav M, Ferreira G, Rosenblum K, Maroun M. 2006. Extinction of conditioned taste aversion depends on functional protein synthesis but not on NMDA receptor activation in the ventromedial prefrontal cortex. *Learn Mem* **13:** 254–258.

Alarcon JM, Malleret G, Touzani K, Vronskaya S, Ishii S, Kandel ER, Barco A. 2004. Chromatin acetylation, memory, and LTP are impaired in CBP+/− mice: a model for the cognitive deficit in Rubinstein–Taybi syndrome and its amelioration. *Neuron* **42:** 947–959.

Allfrey VG, Faulkner R, Mirsky AE. 1964. Acetylation and methylation of histones and their possible role in the regulation of RNA synthesis. *Proc Natl Acad Sci* **51:** 786–794.

Arany Z, Sellers WR, Livingston DM, Eckner R. 1994. E1A-associated p300 and CREB-associated CBP belong to a conserved family of coactivators. *Cell* **77:** 799–800.

Bannister AJ, Kouzarides T. 1996. The CBP co-activator is a histone acetyltransferase. *Nature* **384:** 641–643.

Barrett RM, Malvaez M, Kramar E, Matheos DP, Arrizon A, Cabrera SM, Lynch G, Greene RW, Wood MA. 2011. Hippocampal focal knockout of CBP affects specific histone modifications, long-term potentiation, and long-term memory. *Neuropsychopharmacology* **36:** 1545–1556.

Barrot M, Olivier JD, Perrotti LI, DiLeone RJ, Berton O, Eisch AJ, Impey S, Storm DR, Neve RL, Yin JC, et al. 2002. CREB activity in the nucleus accumbens shell controls gating of behavioral responses to emotional stimuli. *Proc Natl Acad Sci* **99:** 11435–11440.

Blumenfeld RS, Ranganath C. 2007. Prefrontal cortex and long-term memory encoding: an integrative review of findings from neuropsychology and neuroimaging. *Neuroscientist* **13:** 280–291.

Bourtchuladze R, Frenguelli B, Blendy J, Cioffi D, Schutz G, Silva AJ. 1994. Deficient long-term memory in mice with a targeted mutation of the cAMP-responsive element-binding protein. *Cell* **79:** 59–68.

Cetin A, Komai S, Eliava M, Seeburg PH, Osten P. 2006. Stereotaxic gene delivery in the rodent brain. *Nat Protoc* **1:** 3166–3173.

Chen G, Zou X, Watanabe H, van Deursen JM, Shen J. 2010. CREB binding protein is required for both short-term and long-term memory formation. *J Neurosci* **30:** 13066–13077.

Chrivia JC, Kwok RP, Lamb N, Hagiwara M, Montminy MR, Goodman RH. 1993. Phosphorylated CREB binds specifically to the nuclear protein CBP. *Nature* **365:** 855–859.

Dash PK, Hochner B, Kandel ER. 1990. Injection of the cAMP-responsive element into the nucleus of *Aplysia* sensory neurons blocks long-term facilitation. *Nature* **345:** 718–721.

DeVito LM, Lykken C, Kanter BR, Eichenbaum H. 2010. Prefrontal cortex: role in acquisition of overlapping associations and transitive inference. *Learn Mem* **17:** 161–167.

Eckner R, Ewen ME, Newsome D, Gerdes M, DeCaprio JA, Lawrence JB, Livingston DM. 1994. Molecular cloning and functional analysis of the adenovirus E1A-associated 300-kD protein (p300) reveals a protein with properties of a transcriptional adaptor. *Genes Dev* **8:** 869–884.

Fanselow MS. 1980. Conditioned and unconditional components of post-shock freezing. *Pavlov J Biol Sci* **15:** 177–182.

Fanselow MS, LeDoux JE. 1999. Why we think plasticity underlying Pavlovian fear conditioning occurs in the basolateral amygdala. *Neuron* **23:** 229–232.

Glozak MA, Sengupta N, Zhang X, Seto E. 2005. Acetylation and deacetylation of non-histone proteins. *Gene* **363:** 15–23.

Gonzalez GA, Yamamoto KK, Fischer WH, Karr D, Menzel P, Biggs W III, Vale WW, Montminy MR. 1989. A cluster of phosphorylation sites on the cyclic AMP-regulated nuclear factor CREB predicted by its sequence. *Nature* **337:** 749–752.

Gu W, Roeder RG. 1997. Activation of p53 sequence-specific DNA binding by acetylation of the p53 C-terminal domain. *Cell* **90:** 595–606.

Guan Z, Giustetto M, Lomvardas S, Kim JH, Miniaci MC, Schwartz JH, Thanos D, Kandel ER. 2002. Integration of long-term-memory-related synaptic plasticity involves bidirectional regulation of gene expression and chromatin structure. *Cell* **111:** 483–493.

Hirsch JC, Crepel F. 1992. Postsynaptic calcium is necessary for the induction of LTP and LTD of monosynaptic EPSPs in prefrontal neurons: an in vitro study in the rat. *Synapse* **10:** 173–175.

Izaki Y, Takita M, Nomura M. 2002. Local properties of CA1 region in hippocampo-prefrontal synaptic plasticity in rats. *Neuroreport* **13:** 469–472.

Josselyn SA, Shi C, Carlezon WA Jr, Neve RL, Nestler EJ, Davis M. 2001. Long-term memory is facilitated by cAMP response element-binding protein overexpression in the amygdala. *J Neurosci* **21:** 2404–2412.

Karlic R, Chung HR, Lasserre J, Vlahovicek K, Vingron M. 2010. Histone modification levels are predictive for gene expression. *Proc Natl Acad Sci* **107:** 2926–2931.

Kawashima H, Izaki Y, Grace AA, Takita M. 2006. Cooperativity between hippocampal-prefrontal short-term plasticity through associative long-term potentiation. *Brain Res* **1109:** 37–44.

Kesner RP, Rogers J. 2004. An analysis of independence and interactions of brain substrates that subserve multiple attributes, memory systems, and underlying processes. *Neurobiol Learn Mem* **82:** 199–215.

Kida S, Josselyn SA, de Ortiz SP, Kogan JH, Chevere I, Masushige S, Silva AJ. 2002. CREB required for the stability of new and reactivated fear memories. *Nat Neurosci* **5:** 348–355.

Kimura A, Matsubara K, Horikoshi M. 2005. A decade of histone acetylation: marking eukaryotic chromosomes with specific codes. *J Biochem* **138:** 647–662.

Kojima N, Wang J, Mansuy IM, Grant SG, Mayford M, Kandel ER. 1997. Rescuing impairment of long-term potentiation in fyn-deficient mice by introducing Fyn transgene. *Proc Natl Acad Sci* **94:** 4761–4765.

Korzus E, Torchia J, Rose DW, Xu L, Kurokawa R, McInerney EM, Mullen TM, Glass CK, Rosenfeld MG. 1998. Transcription factor-specific requirements for coactivators and their acetyltransferase functions. *Science* **279:** 703–707.

Korzus E, Rosenfeld MG, Mayford M. 2004. CBP histone acetyltransferase activity is a critical component of memory consolidation. *Neuron* **42:** 961–972.

Kouzarides T. 2000. Acetylation: a regulatory modification to rival phosphorylation? *EMBO J* **19:** 1176–1179.

Kumaran D, McClelland JL. 2012. Generalization through the recurrent interaction of episodic memories: a model of the hippocampal system. *Psychol Rev* **119:** 573–616.

Kurdistani SK, Grunstein M. 2003. Histone acetylation and deacetylation in yeast. *Nat Rev Mol Cell Biol* **4:** 276–284.

LeDoux JE. 2000. Emotion circuits in the brain. *Annu Rev Neurosci* **23:** 155–184.

Letzkus JJ, Wolff SB, Meyer EM, Tovote P, Courtin J, Herry C, Luthi A. 2011. A disinhibitory microcircuit for associative fear learning in the auditory cortex. *Nature* **480:** 331–335.

Leutgeb JK, Leutgeb S, Moser MB, Moser EI. 2007. Pattern separation in the dentate gyrus and CA3 of the hippocampus. *Science* **315:** 961–966.

Lim F, Neve RL. 2001. Generation of high-titer defective HSV-1 vectors. *Curr Protoc Neurosci* Chapter 4: Unit 4 13.

Lopez-Atalaya JP, Ciccarelli A, Viosca J, Valor LM, Jimenez-Minchan M, Canals S, Giustetto M, Barco A. 2011. CBP is required for environmental enrichment-induced neurogenesis and cognitive enhancement. *EMBO J* **30:** 4287–4298.

Lovelace JW, Vieira PA, Corches A, Mackie K, Korzus E. 2014. Impaired fear memory specificity associated with deficient endocannabinoid-dependent long-term plasticity. *Neuropsychopharmacology* **39:** 1685–1693.

Lu Q, Hutchins AE, Doyle CM, Lundblad JR, Kwok RP. 2003. Acetylation of cAMP-responsive element-binding protein (CREB) by CREB-binding protein enhances CREB-dependent transcription. *J Biol Chem* **278:** 15727–15734.

Maddox SA, Watts CS, Schafe GE. 2013. p300/CBP histone acetyltransferase activity is required for newly acquired and reactivated fear memories in the lateral amygdala. *Learn Mem* **20:** 109–119.

Mahan AL, Ressler KJ. 2012. Fear conditioning, synaptic plasticity and the amygdala: implications for posttraumatic stress disorder. *Trends Neurosci* **35:** 24–35.

Markowetz F, Mulder KW, Airoldi EM, Lemischka IR, Troyanskaya OG. 2010. Mapping dynamic histone acetylation patterns to gene expression in nanog-depleted murine embryonic stem cells. *PLoS Comput Biol* **6:** e1001034.

Maroun M, Richter-Levin G. 2003. Exposure to acute stress blocks the induction of long-term potentiation of the amygdala-prefrontal cortex pathway in vivo. *J Neurosci* **23:** 4406–4409.

Marr D. 1971. Simple memory: a theory for archicortex. *Philos Trans R Soc Lond B Biol Sci* **262:** 23–81.

McHugh TJ, Jones MW, Quinn JJ, Balthasar N, Coppari R, Elmquist JK, Lowell BB, Fanselow MS, Wilson MA, Tonegawa S. 2007. Dentate gyrus NMDA receptors mediate rapid pattern separation in the hippocampal network. *Science* **317:** 94–99.

Morris SH, Knevett S, Lerner EG, Bindman LJ. 1999. Group I mGluR agonist DHPG facilitates the induction of LTP in rat prelimbic cortex in vitro. *J Neurophysiol* **82:** 1927–1933.

Nakashiba T, Cushman JD, Pelkey KA, Renaudineau S, Buhl DL, McHugh TJ, Rodriguez Barrera V, Chittajallu R, Iwamoto KS, McBain CJ, et al. 2012. Young dentate granule cells mediate pattern separation, whereas old granule cells facilitate pattern completion. *Cell* **149:** 188–201.

Navawongse R, Eichenbaum H. 2013. Distinct pathways for rule-based retrieval and spatial mapping of memory representations in hippocampal neurons. *J Neurosci* **33:** 1002–1013.

Neve RL, Lim F. 2001. Overview of gene delivery into cells using HSV-1-based vectors. *Curr Protoc Neurosci* **Chapter 4:** Unit 4 12.

Ogryzko VV, Schiltz RL, Russanova V, Howard BH, Nakatani Y. 1996. The transcriptional coactivators p300 and CBP are histone acetyltransferases. *Cell* **87:** 953–959.

Olson VG, Zabetian CP, Bolanos CA, Edwards S, Barrot M, Eisch AJ, Hughes T, Self DW, Neve RL, Nestler EJ. 2005. Regulation of drug reward by cAMP response element-binding protein: evidence for two functionally distinct subregions of the ventral tegmental area. *J Neurosci* **25:** 5553–5562.

O'Reilly RC, McClelland JL. 1994. Hippocampal conjunctive encoding, storage, and recall: avoiding a trade-off. *Hippocampus* **4:** 661–682.

Paxinos G, Franklin KBJ. 2001. *The mouse brain in stereotaxic coordinates*. Academic Press, San Diego, CA.

Peixoto L, Abel T. 2012. The role of histone acetylation in memory formation and cognitive impairments. *Neuropsychopharmacology* **38:** 62–76.

Petrij F, Giles RH, Dauwerse HG, Saris JJ, Hennekam RC, Masuno M, Tommerup N, van Ommen GJ, Goodman RH, Peters DJ, et al. 1995. Rubinstein–Taybi syndrome caused by mutations in the transcriptional co-activator CBP. *Nature* **376:** 348–351.

Pittenger C, Huang YY, Paletzki RF, Bourtchouladze R, Scanlin H, Vronskaya S, Kandel ER. 2002. Reversible inhibition of CREB/ATF transcription factors in region CA1 of the dorsal hippocampus disrupts hippocampus-dependent spatial memory. *Neuron* **34:** 447–462.

Pogo BG, Allfrey VG, Mirsky AE. 1966. RNA synthesis and histone acetylation during the course of gene activation in lymphocytes. *Proc Natl Acad Sci* **55:** 805–812.

Puri PL, Sartorelli V, Yang XJ, Hamamori Y, Ogryzko VV, Howard BH, Kedes L, Wang JY, Graessmann A, Nakatani Y, et al. 1997. Differential roles of p300 and PCAF acetyltransferases in muscle differentiation. *Mol Cell* **1:** 35–45.

Quirk GJ, Mueller D. 2008. Neural mechanisms of extinction learning and retrieval. *Neuropsychopharmacology* **33:** 56–72.

Quirk GJ, Russo GK, Barron JL, Lebron K. 2000. The role of ventromedial prefrontal cortex in the recovery of extinguished fear. *J Neurosci* **20:** 6225–6231.

Richter-Levin G, Maroun M. 2010. Stress and amygdala suppression of metaplasticity in the medial prefrontal cortex. *Cereb Cortex* **20:** 2433–2441.

Rogerson T, Cai DJ, Frank A, Sano Y, Shobe J, Lopez-Aranda MF, Silva AJ. 2014. Synaptic tagging during memory allocation. *Nat Rev Neurosci* **15:** 157–169.

Rosenfeld MG, Glass CK. 2001. Coregulator codes of transcriptional regulation by nuclear receptors. *J Biol Chem* **276:** 36865–36868.

Rubinstein JH, Taybi H. 1963. Broad thumbs and toes and facial abnormalities. A possible mental retardation syndrome. *Am J Dis Child* **105:** 588–608.

Sahay A, Wilson DA, Hen R. 2011. Pattern separation: a common function for new neurons in hippocampus and olfactory bulb. *Neuron* **70:** 582–588.

Santini E, Ge H, Ren K, Pena de Ortiz S, Quirk GJ. 2004. Consolidation of fear extinction requires protein synthesis in the medial prefrontal cortex. *J Neurosci* **24:** 5704–5710.

Sotres-Bayon F, Cain CK, LeDoux JE. 2006. Brain mechanisms of fear extinction: historical perspectives on the contribution of prefrontal cortex. *Biol Psychiatry* **60:** 329–336.

Sterner DE, Berger SL. 2000. Acetylation of histones and transcription-related factors. *Microbiol Mol Biol Rev* **64:** 435–459.

Sugiura H, Yamauchi T. 1992. Developmental changes in the levels of Ca^{2+}/calmodulin-dependent protein kinase II α and β proteins in soluble and particulate fractions of the rat brain. *Brain Res* **593:** 97–104.

Takita M, Izaki Y, Jay TM, Kaneko H, Suzuki SS. 1999. Induction of stable long-term depression in vivo in the hippocampal–prefrontal cortex pathway. *Eur J Neurosci* **11:** 4145–4148.

Valor LM, Pulopulos MM, Jimenez-Minchan M, Olivares R, Lutz B, Barco A. 2011. Ablation of CBP in forebrain principal neurons causes modest memory and transcriptional defects and a dramatic reduction of histone acetylation but does not affect cell viability. *J Neurosci* **31:** 1652–1663.

Valor LM, Viosca J, Lopez-Atalaya JP, Barco A. 2013. Lysine acetyltransferases CBP and p300 as therapeutic targets in cognitive and neurodegenerative disorders. *Curr Pharm Des* **19:** 5051–5064.

Vogel-Ciernia A, Matheos DP, Barrett RM, Kramar EA, Azzawi S, Chen Y, Magnan CN, Zeller M, Sylvain A, Haettig J, et al. 2013. The neuron-specific chromatin regulatory subunit BAF53b is necessary for synaptic plasticity and memory. *Nat Neurosci* **16:** 552–561.

Wood MA, Kaplan MP, Park A, Blanchard EJ, Oliveira AM, Lombardi TL, Abel T. 2005. Transgenic mice expressing a truncated form of CREB-binding protein (CBP) exhibit deficits in hippocampal synaptic plasticity and memory storage. *Learn Mem* **12:** 111–119.

Xu W, Sudhof TC. 2013. A neural circuit for memory specificity and generalization. *Science* **339:** 1290–1295.

Xu W, Morishita W, Buckmaster PS, Pang ZP, Malenka RC, Sudhof TC. 2012. Distinct neuronal coding schemes in memory revealed by selective erasure of fast synchronous synaptic transmission. *Neuron* **73:** 990–1001.

Yang XJ. 2004. Lysine acetylation and the bromodomain: a new partnership for signaling. *Bioessays* **26:** 1076–1087.

Yao TP, Oh SP, Fuchs M, Zhou ND, Ch'ng LE, Newsome D, Bronson RT, Li E, Livingston DM, Eckner R. 1998. Gene dosage-dependent embryonic development and proliferation defects in mice lacking the transcriptional integrator p300. *Cell* **93:** 361–372.

Yin JC, Wallach JS, Del Vecchio M, Wilder EL, Zhou H, Quinn WG, Tully T. 1994. Induction of a dominant negative CREB transgene specifically blocks long-term memory in *Drosophila*. *Cell* **79:** 49–58.

Zeng FG, Nie K, Stickney GS, Kong YY, Vongphoe M, Bhargave A, Wei C, Cao K. 2005. Speech recognition with amplitude and frequency modulations. *Proc Natl Acad Sci* **102:** 2293–2298.